Sporadic-E morphology from 13 years of COSMIC-1

Björn Bergsson[1] and Stig Syndergaard[2]

[1]Embry-Riddle Aeronautical University, Daytona Beach, Florida, USA

[2]Danish Meteorological Institute, Copenhagen, Denmark

Abstract

We have analyzed 13 years of radio occultation data from the first Constellation Observing System for Meteorology, Ionosphere, and Climate (COSMIC-1) mission with a focus on scintillations originating in ionospheric sporadic-E (Es) layers. To identify the Es irregularities, we applied the algorithm developed by Zeng and Sokolovskiy (2010). The analysis enabled the statistical global mapping of Es occurrence in space and time at very high resolution, and allowed an investigation of the statistical variation of Es height and thickness with seasons, solar activity, local time, and latitude. Important new results are that Es height and thickness varies with seasons and solar activity, with different behavior in the morning and in the evening. The evening Es height and thickness varies significantly with solar activity, apparently having lower mean height and larger mean thickness when the activity is high. We interpret that as a tendency for the evening Es to be more tilted with respect to the local horizon.

Theory

Es irregularities have previously been modeled by Zeng and Sokolovskiy (2010) as horizontally elongated structures of vertical thickness up to a few km with a vertical electron density gradient increasing towards the middle. When a signal travels through such an Es cloud that is aligned with the propagation direction, bending of the signal path happens outwards from the middle.

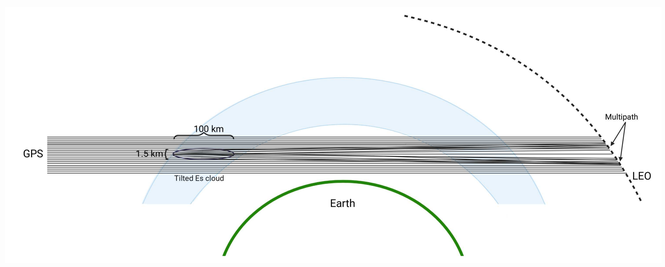

Figure 1: At low tangent heights, the signal propagation through the Es cloud results in multipath interference if the cloud is tilted w.r.t. its local horizon.

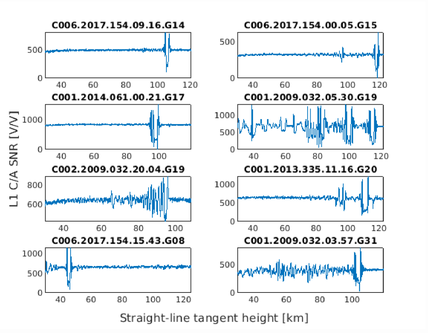

Figure 2: The multipath interference results in a U-shape structure in the COSMIC-1 SNR.

Method

To identify the Es irregularities, an algorithm developed by Zeng and Sokolovskiy (2010) is used which is specifically designed to detect U-shape structures in the SNR. It estimates the depth and the multipath interference effects seen in the U-shape, and makes an Es detection if the following two criteria are met:

1. $A_{1\mathrm{km}} < 0.6 \cdot A_{20\mathrm{km}}$.
2. The standard deviation of the amplitude fluctuations calculated in the center of the U-shape structure is smaller than the standard deviation of the fluctuations at both sides of the U-shape, and at least three times smaller than any one of them.

Given an Es detection, the thickness of the cloud is determined by the interval where $A_{1\mathrm{km}} < 0.95 \cdot A_{20\mathrm{km}}$, and the height of the cloud is determined by the middle of the interval.

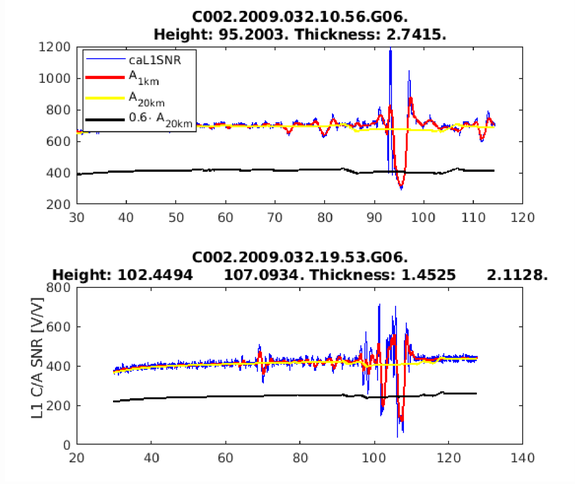

Figure 3: Examples of how the U-shape algorithm detects Es in COSMIC-1 profiles.

Es-layer height, thickness, spatial, and local time distribution

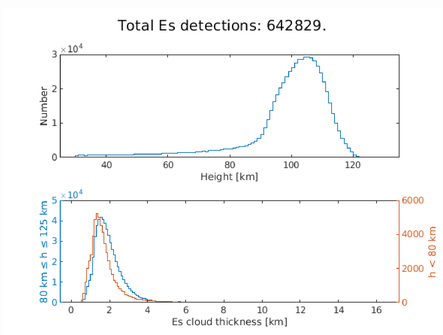

Figure 4: Distributions of Es in height and thickness in COSMIC-1 data from years 2007-2019. (Bin size 1 km in height and 0.1 km in thickness). The distribution in thickness is split according to detections above and below 80 km, meaning it differs between horizontal clouds and tilted clouds.

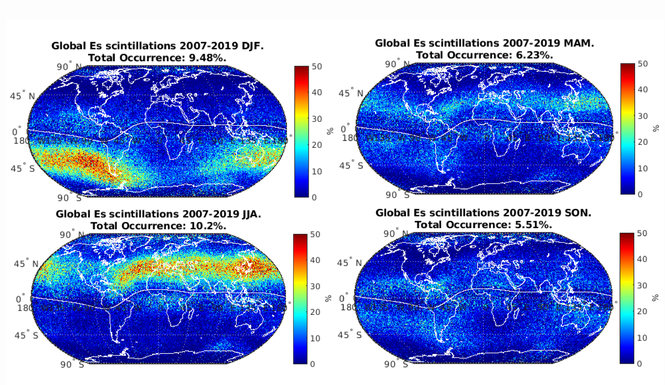

Figure 5: Global maps of Es occurrence rates divided into seasons, with data from 2007-2019. Resolution $1^\circ \times 1^\circ$. The features in Es spatial distribution confirm observations made in previous studies (Wu et al., 2005; Chu et al., 2014; Niu, 2021).

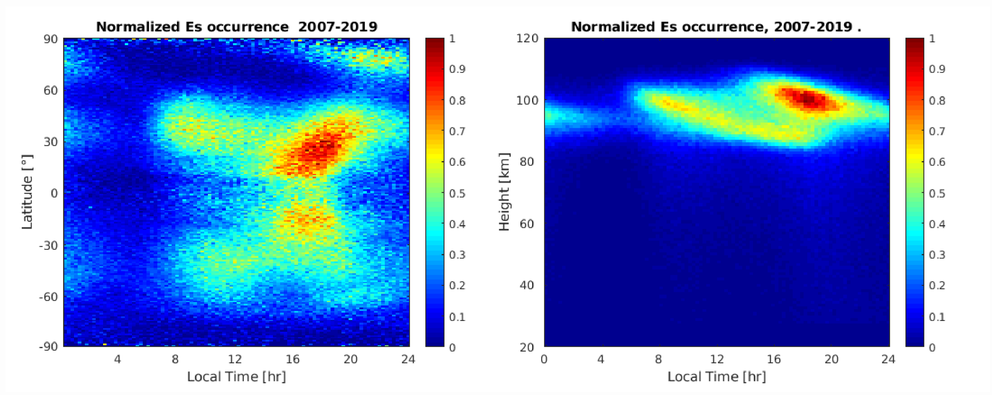

Figure 6: Evolution of Es latitude and height with local time. Resolution $1^\circ \times 15$ min in latitude map and 1 km $\times$ 15 min in height map. It can further be seen by splitting the latitude versus local time map into seasons that the semi-diurnal variations only occur in the summer hemisphere, while the winter hemisphere exhibits diurnal variation (Bergsson and Syndergaard, 2022). This is in accordance with results in previous studies (Wu et al., 2005; Wu, 2020).

Es variations with Seasons and Solar Activity

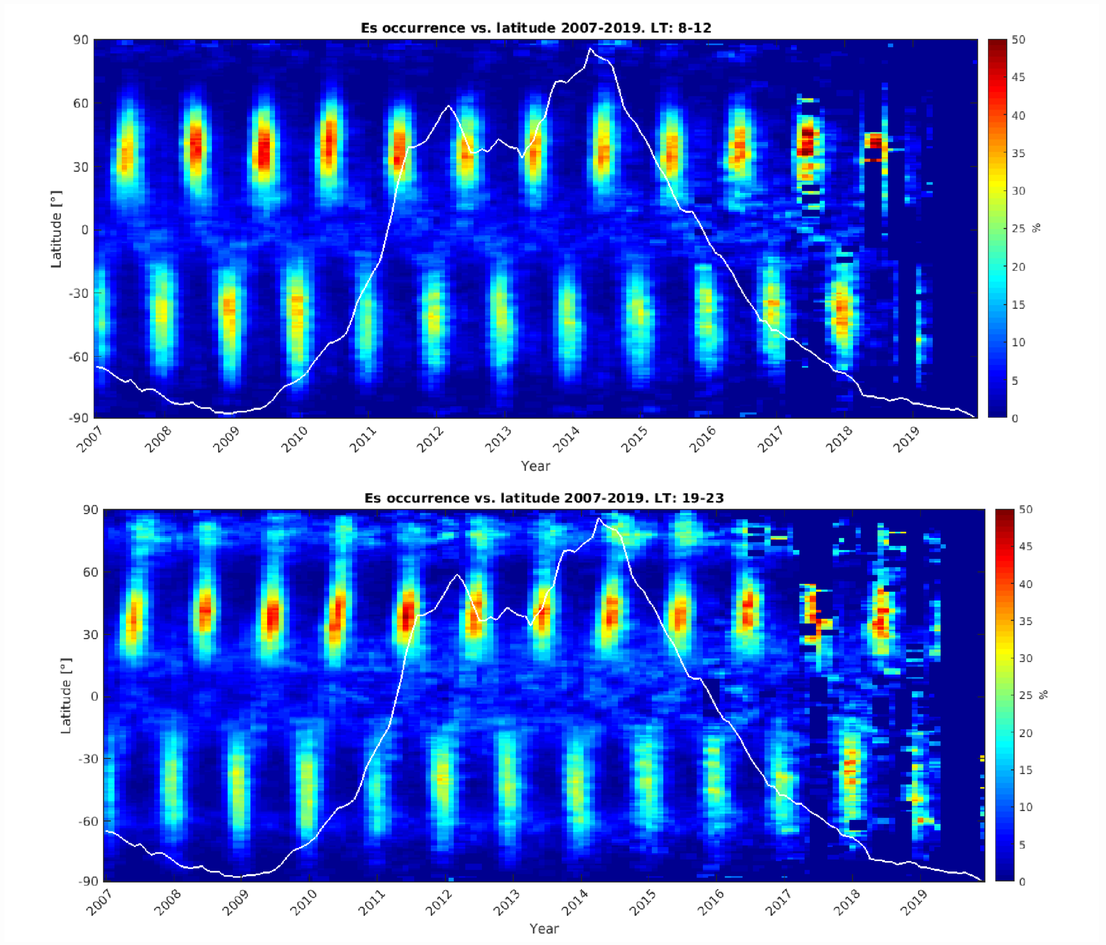

Figure 7: The Es occurrence shown in a monthly mean time series for years 2007-2019, split into morning (upper) and evening (lower) local times. Maps smoothed with 3×3 box filter to better observe the patterns. Resolution $1^\circ \times 1$ month. The superimposed white line is the scaled running mean sunspot number which denotes the solar activity over the years. At mid-latitudes, anti-correlation with solar activity is seen more clearly at morning times. However, only at evening times, the Es occurrence appears to be correlated with solar activity at low latitudes, and Es activity is observed over the poles. It should be noted that although the map extends to the end of 2019 we observe some data gaps in the later years. That is because as the COSMIC-1 flight modules and their sensors gradually malfunctioned, the sampling decreased, and uniform sampling was not quite obtained after 2016 (Wu, 2020). Therefore, for the later years where sampling is low, the results are not as reliable.

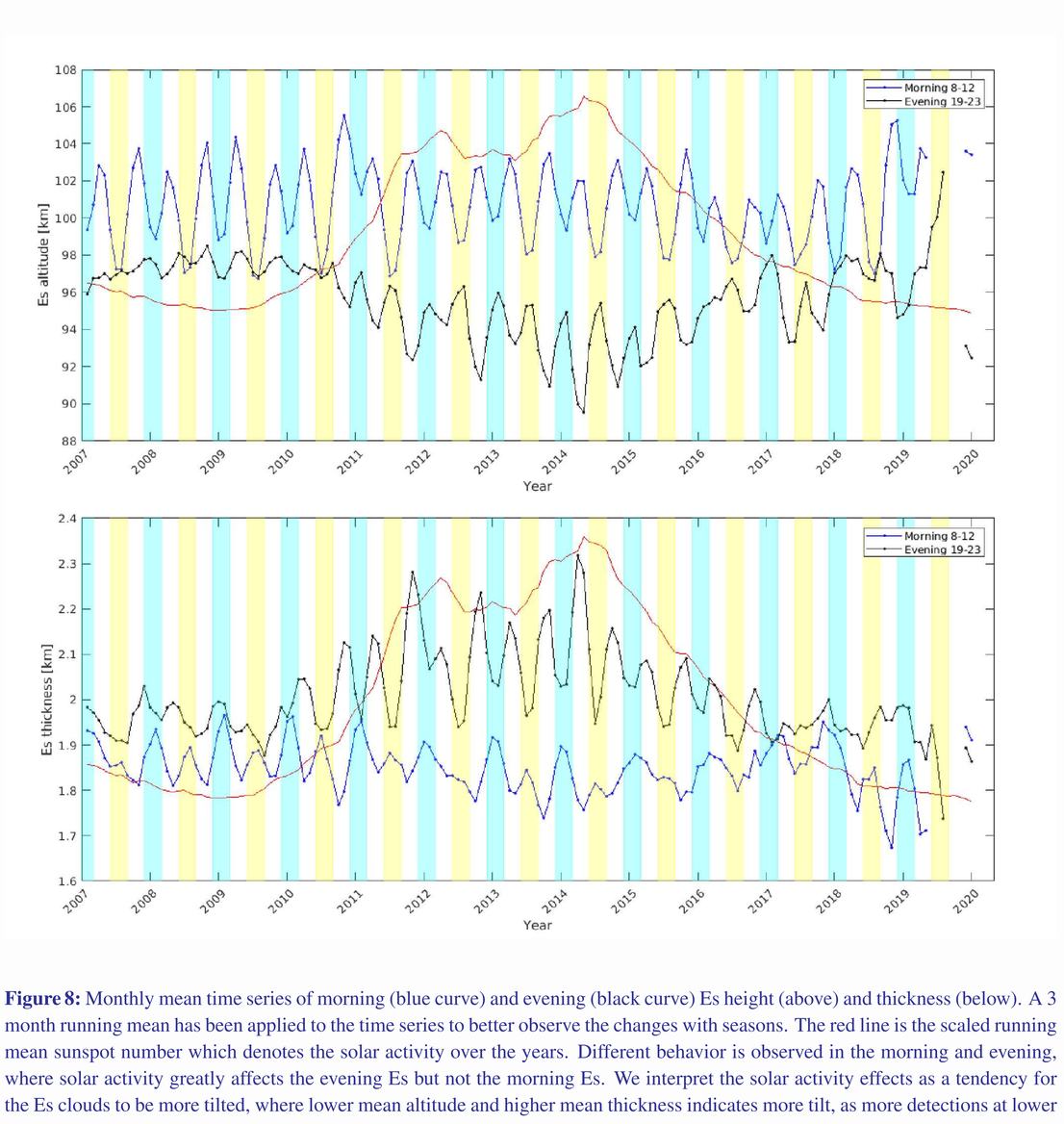

Figure 8: Monthly mean time series of morning (blue curve) and evening (black curve) Es height (above) and thickness (below). A 3 month running mean has been applied to the time series to better observe the changes with seasons. The red line is the scaled running mean sunspot number which denotes the solar activity over the years. Different behavior is observed in the morning and evening, where solar activity greatly affects the evening Es but not the morning Es. We interpret the solar activity effects as a tendency for the Es clouds to be more tilted, where lower mean altitude and higher mean thickness indicates more tilt, as more detections at lower height of greater thickness are made because the clouds are more aligned with the signal propagation direction. Further research suggests that it is the evening Es at low latitudes that gets affected by solar activity in this way (Bergsson and Syndergaard (2022)).

References

Bergsson, B. and S. Syndergaard, 2022: Global temporal and spatial variations of ionospheric sporadic-E derived from radio occultation measurements. *Journal of Geophysical Research: Space Physics*, **127**, e2022JA030296, doi:10.1029/2022JA030296.

Chu, Y. H., C. Y.Wang, K. H. Wu, K. T. Chen, K. J. Tzeng, C. L. Su, W. Feng, and J. M. C. Plane, 2014: Morphology of sporadic E layer retrieved from COSMIC GPS radio occultation measurements: Wind shear theory examination. *J. Geophys. Res. Space Physics*, **119**, 2117–2136, doi:10.1002/2013JA019437.

Niu, J., 2021: Difference in the sporadic E layer occurrence ratio between the southern and northern low magnetic latitude regions as observed by COSMIC radio occultation data. *Space Weather*, **19**, doi:10.1029/2020SW002635.

Wu, D. L., 2020: Ionospheric S4 scintillations from GNSS radio occultation (RO) at slant path. *Remote Sensing*, **12**, 2373, doi:10.3390/rs12152373.

Wu, D. L., C. O. Ao, G. A. Hajj, M. de la Torre Juarez, and A. J. Mannucci, 2005: Sporadic E morphology from GPS-CHAMP radio occultation. *Journal of Geophysical Research*, **110**, doi:10.1029/2004JA010701.

Zeng, Z. and S. Sokolovskiy, 2010: Effect of sporadic E clouds on GPS radio occultation signals. *Geophys. Res. Lett.*, **37, L18817**, doi:10.1029/2010GL044561.